Solid State Structures and Dynamic Solution Equilibria of Bis(dibenzylamido)magnesium Complexes: Aggregation Dependence on Stoichiometry and Denticity of Donor Solvent

William Clegg,[†] Fiona J. Craig,[‡] Kenneth W. Henderson,*[,‡] Alan R. Kennedy,[‡] Robert E. Mulvey,*[,‡] Paul A. O'Neil,[†] and David Reed[§]

Department of Chemistry, University of Newcastle-upon-Tyne, Newcastle NE1 7RU, U.K., Department of Pure and Applied Chemistry, University of Strathclyde, Glasgow G1 1XL, U.K., and Department of Chemistry, University of Edinburgh, Edinburgh EH9 3JJ, U.K.

Received July 24, 1997[⊗]

Reaction of commercial Bu_2Mg with 2 molar equiv of dibenzylamine gives the bis(amido)magnesium complex $[\{\{(PhCH_2)_2N\}_2Mg\}_2]$, **1**. Compound **1** is dimeric with three-coordinate magnesium in the crystalline state. Addition of 2 molar equiv of the monodentate donor solvents THF and HMPA to solutions of **1** affords the complexes $[\{\{(PhCH_2)_2N\}_2Mg\cdot THF\}_2]$, **2**, and $[\{\{(PhCH_2)_2N\}_2Mg\cdot HMPA\}_2]$, **4** respectively, which maintain the dimeric framework but increase the metal's coordination number to 4. Addition of 4 molar equiv of HMPA, or a 20-fold excess, of THF to **1** causes deaggregation of the dimer to the monomeric bis-solvates $[\{(PhCH_2)_2N\}_2Mg\cdot 2THF]$, **3**, and $[\{(PhCH_2)_2N\}_2Mg\cdot 2HMPA]$, **5**. The chelating ligand TMEDA gives the monomer $[\{(PhCH_2)_2N\}_2Mg\cdot TMEDA]$, **6**, on mixing with **1**. ^1H and ^{13}C NMR spectroscopic studies reveal that dimer **1** is partially retained in arene solution but is in equilibrium with the unsolvated monomer $[\{(PhCH_2)_2N\}_2Mg]$, **7**. Concentration studies on solutions of monosolvated dimer **4** show it to be in equilibrium with both the bis-solvated monomer **5** and the unsolvated monomer **7**. X-ray crystallographic determinations have been carried out on complexes **1**, **2**, and **4**−**6**, and a comparative analysis of their structures is detailed. The bis(dibenzylamido)-magnesium system has shown remarkable structural flexibility with di-, tri-, and tetracoordination at the metal.

Introduction

(Amido)magnesium (R_2NMgX, where X = organyl, amide, alkoxide, *etc.*) chemistry is becoming an increasingly active area of study.[1] In part, this is due to the status gained by lithium amide complexes as reagents in synthesis.[2] Being lithium's diagonal neighbor, magnesium is clearly of interest since its complexes may offer differing selectivities and reactivities compared with the lithium derivatives. For example, anti selectivity in aldol reactions can be achieved using the Hauser base chloromagnesium diisopropylamide (Pr^i_2NMgCl) under thermodynamic conditions (up to 98:2 anti/syn aldolate), in good to high yields.[3] In comparison, thermodynamic equilibration of lithium aldolates is often complicated by the retro-aldol reaction, resulting in lower yields.[4] Clearly, a better understanding of the (amido)magnesium species that are involved in such reactions would be advantageous. To date, the reactivity and coordination chemistry of bis(amido)magnesium compounds[5] has been eclipsed by that of the more widely utilized Grignard reagents.[6]

We recently detailed the dismutation reaction of alkyl(amido)-magnesium compounds containing a 2-pyridyl unit into their bis(amido) and bis(alkyl) derivatives.[7] A highlight arising from this investigation is the solvent dependency of the equilibrium depicted in eq 1.

$$2R(2\text{-pyr})NMgR' \overset{\text{solvent (S)}}{\rightleftharpoons} [\{R(2\text{-pyr})N\}_2Mg\cdot xS] + [R'_2Mg\cdot xS] \quad (1)$$

$$R = \text{alkyl or aryl; } R' = Bu$$

The introduction of donor solvents such as tetrahydrofuran (THF), hexamethylphosphoramide (HMPA), and *N*,*N*,*N*′,*N*′-tetramethylethylenediamine (TMEDA) drives the reaction to the homoleptic components by maximizing the coordination environment around the metal center. Overall, there is an increase

[†] University of Newcastle-upon-Tyne.
[‡] University of Strathclyde.
[§] University of Edinburgh.
[⊗] Abstract published in *Advance ACS Abstracts,* December 15, 1997.

(1) (a) Bonafoux, D.; Bordeau, M.; Biran, C.; Cazeau, P.; Dunogues, J. *J. Org. Chem.* **1996**, *61*, 5532. (b) Kondo, Y.; Yoshida, A.; Sakamoto, T. *J. Chem. Soc., Perkin Trans.* **1996**, 2331. (c) Kobayashi, K.; Yokota, K.; Akamatsu, H.; Morikawa, O; Konishi, H. *Bull. Chem. Soc. Jpn.* **1996**, *69*, 441. (d) Kobaiyashi, K.; Kawakita, M.; Mannami, T.; Morikawa, O.; Konishi, H. *Chem. Lett.* **1994**, 1551. (e) Van Draanen, N. A.; Arseniyadis, S.; Crimmins, M. T.; Heathcock, C. H. *J. Org. Chem.* **1991**, *56*, 2499. (f) Eaton, P. E.; Lee, C. H.; Xiong, Y. *J. Am. Chem. Soc.* **1989**, *111*, 8016.

(2) For reviews of lithium amides as reagents in organic synthesis, see: (a) Snieckus, V. *Chem. Rev.* **1990**, *90*, 879. (b) Evans, D. In *Asymmetric Synthesis*; Morrison, J. D., Ed.; Academic Press: New York, 1983; Vol. 3, Chapter 1; also see Vols. 1 and 2. (c) Simpkins, N. S. *Tetrahedron: Asymmetry* **1991**, *2*, 1. (d) d'Angelo, J. *Tetrahedron* **1976**, *32*, 2979. (e) Heathcock, C. H. In *Comprehensive Carbanion Chemistry*; Buncel, E., Durst, T., Eds.; Elsevier: New York, 1980.

(3) Swiss, K. A.; Woo-Baeg, C.; Liotta. D. C.; Abdel-Magrid, A. F.; Maryanoff, C. A. *J. Org. Chem.* **1991**, *56*, 5978.

(4) Heathcock, C. H.; Buse, C. T.; Kleschick, W. A.; Pirrung, M. C.; Sohn, J. E.; Lampe, J. *J. Org. Chem.* **1980**, *45*, 1066.

(5) (a) Lappert, M. F.; Power, P. P.; Sanger, A. R.; Srivastava, R. C. *Metal and Metalloid Amides*; Ellis Horwood: Chichester, U.K., 1980. (b) Veith, M. *Adv. Organomet. Chem.* **1990**, *31*, 269. (c) Pinkus, A. G. *Coord. Chem. Rev.* **1978**, *25*, 173. (d) Duff, A. W.; Hitchcock, P. B.; Lappert, M. F.; Taylor R. G.; Segal, J. A. *J. Organomet. Chem.* **1985**, *293*, 271. (e) Holloway, C. E.; Melnik, M. *J. Organomet. Chem.* **1994**, *465*, 1. (f) For a review of the early work on alkyl(amido)magnesiums, see: Wakefield, B. J. *Adv. Inorg. Chem. Radiochem.* **1968**, *11*, 341.

(6) (a) Wakefield, B. J. *Organomagnesium Methods in Organic Synthesis*; Academic Press: New York, 1995. (b) Lindsell, W. E. In *Comprehensive Organometallic Chemistry*; Wilkinson, G., Stone, F. G. A., Abel, E. W., Eds.; Pergamon Press: Oxford, U.K., 1982; Vol. 1, Chapter 4. (c) Heathcock, C. H. In *Comprehensive Organic Chemistry*; Trost, B. M., Flemming, I. Eds.; Pergamon Press: Oxford, U.K., 1991; Vol. 2, Chapter 1.6.

(7) (a) Henderson, K. W.; Mulvey, R. E.; Dorigo, A. E. *J. Organomet. Chem.* **1996**, *518*, 139. (b) Henderson, K. W.; Mulvey, R. E.; O'Neil, P. A.; Clegg, W. *J. Organomet. Chem.* **1992**, *439*, 237.

S0020-1669(97)00912-9 CCC: $14.00

in coordination number at the metal, from 4 in the alkyl(amido)-magnesium (which exists as a solvent-free chelated dimer) to 6 in the bis-solvated bis(amido) monomer. The increase in coordination number for the bis(amide) is possible due to the low steric requirements of the anion.

We now report our findings on the solvent-dependent aggregation and coordination of bis(dibenzylamido)magnesium complexes, [{$(PhCH_2)_2N$}$_2$Mg]. Previously the dibenzylamido anion has been used extensively with group 1 metals to elucidate aspects of their fundamental coordination chemistry.[8]

Experimental Section

All experimental manipulations were performed under an argon atmosphere using standard Schlenk techniques[9] or in an argon-filled glovebox. All solvents were distilled from sodium/benzophenone and stored over 4A molecular sieves. HMPA, TMEDA, and dibenzylamine (DBA) were stored over 4A molecular sieves prior to use. Bu_2Mg was used as received from Aldrich as a 1 M solution in heptane. IR spectra were run on a Perkin-Elmer 457 spectrometer as Nujol mulls on NaCl plates. NMR data were obtained on a Bruker AMX 400 spectrometer, and variable-temperature studies were performed on a Bruker WH360 spectrometer. NMR spectra were run at 298 K unless otherwise stated and internally referenced to the deuterated solvent. All samples were dissolved in C_6D_6 except **1**, which was dissolved in C_7D_8 due to improved solubility. Samples with inconclusive NMR data were also investigated as THF-d_8 solutions to reduce the complexity of variable aggregation states.

[{{$(PhCH_2)_2N$}$_2$Mg}$_2$] (1). A Schlenk tube was charged with Bu_2-Mg (10 mmol), and the heptane solvent was removed under vacuum. The residual oil was dissolved in 10 mL of toluene, and DBA (20 mmol) was added dropwise to the resultant solution. Large crystalline blocks of **1** were deposited on standing at ambient temperature for 12 h. Yield = 61%. Mp = 175−177 °C. IR (cm^{-1}): 2920 (s), 2870 (s), 1450 (m), 1376 (w), 1342 (w), 1237 (w), 1180 (w), 1140 (w), 1050 (w), 1005 (w), 950 (m), 901 (w), 749 (m), 726 (m), 700 (m), 441 (w). ^{1}H NMR (δ) in C_7H_8: 2.73 (2H, broad s, PhCH_2), 3.98 (2H, broad s, PhCH_2), 6.80−7.45 (series of multiplets, 10H, *Ph*). ^{13}C NMR (δ) in C_7H_8: 53.52 (PhCH_2), 125.40−129.16 (series of overlapping signals, *Ph*), 141.19 (*ipso-C*). ^{1}H NMR (δ) in THF-d_8: 3.97 (4H, s, PhCH_2), 7.05 (t, 2H, *p-H*), 7.19 (t, 4H, *m-H*), 7.36 (d, 4H, *o-H*). ^{13}C NMR (δ) in THF-d_8: 58.30 (PhCH_2), 125.80 (*p-H*), 128.80 (*o-C*), 129.13 (*m-C*), 148.29 (*i-C*).

[{{$(PhCH_2)_2N$}$_2$Mg·THF}$_2$] (2). THF (10 mmol) was added slowly to a solution of **1** (5 mmol) in 8 mL of toluene with no visible change in the reaction mixture. Cooling the solution to 0 °C for 12 h yielded a white solid. The solid was dissolved on heating to ∼60 °C, and crystals of **2** precipitated upon slow cooling of this solution to ambient temperature over 6 h. Yield = 40%. Mp = 118−119 °C. IR (cm^{-1}): 2920 (s), 2890 (s), 2800 (w), 2755 (w), 2675 (w), 1603 (w), 1487 (s), 1470 (m), 1447 (s), 1379 (w), 1370 (w), 1358 (m), 1190 (w), 1183 (m), 1119 (m), 1099 (w), 1070 (m), 1051 (w), 1023 (m), 945 (m), 928 (w), 890 (w), 736 (s), 725 (s), 698 (s), 636 (w), 539 (w), 521 (w), 469 (m). ^{1}H NMR (δ) in C_6D_6: 1.08 (s, 4H, C$H_2$$CH_2O$), 3.55 (s, 4H, C$H_2$O), 4.18 (s, 8H, C$H_2$Ph), 7.04 (m, 4H, *p-H*), 7.25 (t, 8H, *m-H*), 7.42 (d, 8H, *o-H*). ^{13}C NMR (δ) in C_6D_6: 25.35 (*C*$H_2$$CH_2O$), 69.63 (*C*$H_2$O), 56.22 (*C*$H_2$Ph), 126.93 (*p-C*), 128.79 (*o-C*), 129.16 (*m-C*), 144.75 (*i-C*).

[{$(PhCH_2)_2N$}$_2$Mg·(THF)$_2$] (3). THF (100 mmol) was added to a solution of **1** (5 mmol) in 10 mL of toluene. When this solution was cooled at −31 °C for 12 h, a light orange solid was deposited. Attempts at crystallization of this material were unsuccessful. Yield = 68%. Mp = 123−124 °C. IR (cm^{-1}): 2900 (s), 2797 (w), 2755 (w), 1602 (w), 1488 (m), 1448 (s), 1380 (m), 1358 (m), 1343 (w), 1306 (w), 1190 (w), 1182 (w), 1155 (w), 1120 (m), 1098 (w), 1070 (m), 1051 (w), 1022 (m), 981 (w), 951 (w), 946 (m), 946 (m), 930 (w), 890 (m), 736 (s), 725 (s), 698 (s), 636 (m), 538 (w), 520 (w), 468 (m), 433 (w), 398 (w). ^{1}H NMR (δ) in C_6D_6: 1.15 (s, 4H, C$H_2$$CH_2O$), 3.54 (s, 4H, C$H_2$O), 4.60 (s, 4H, C$H_2$Ph), 7.10 (t, 2H, *p-H*), 7.27 (t, 48H, *m-H*), 7.43 (d, 4H, *o-H*). ^{13}C NMR (δ) in C_6D_6: 25.52 (*C*$H_2$$CH_2O$), 69.32 (*C*$H_2$O), 55.99 (*C*$H_2$Ph), 126.74 (*p-C*), 128.80 (*o-C*), 128.95 (*m-C*), 144.64 (*i-C*).

[{{$(PhCH_2)_2N$}$_2$Mg·HMPA}$_2$] (4). Addition of HMPA (10 mmol) to a solution of **1** (5 mmol) in 10 mL of toluene gave an instant color change from pale yellow to red. Slow cooling to 0 °C yielded needle crystals. Yield = 32%. Mp = 108−110 °C. IR (cm^{-1}): 2900 (s), 2755 (m), 2655 (m), 1598 (w), 1486 (m), 1450 (s), 1378 (m), 1353 (m), 1342 (w), 1300 (m), 1190 (s), 1165 (s), 1122 (m), 1090 (w), 1067 (m), 1024 (w), 980 (s), 947 (m), 904 (w), 809 (w), 744 (s), 698 (s), 659 (w), 602 (s), 534 (w), 510 (w), 485 (m), 448 (w). ^{1}H NMR (δ) in C_6D_6: 2.00 (d, NCH_3), 2.25 (d, NCH_3), 4.52 (d, 2H, PhCH_2), 4.72 (s, 4H, PhCH_2), 4.83 (d, 2H, PhCH_2), 7.00−7.36 (m, 12H, *m-H*/*p-H*), 7.67 (d, 4H, *o-H*), 7.76 (d, 4H, *o-H*). ^{13}C NMR (δ) in C_6D_6: 37.07 (NCH_3), 53.78 (PhCH_2), 57.90 (PhCH_2), 128.19 (*p-C*), 129.76 (*o-C*), 130.71 (*m-C*), 143.47 (*i-C*), 147.56 (*i-C*), small signals at 36.80, 36.85, 53.78, 57.45, 125.16−129.90. ^{1}H NMR (δ) in THF-d_8: 2.52 (d, 18H, NCH_3), 3.94 (s, 8H, PhCH_2), 6.95 (t, 4H, *p-H*), 7.09 (t, 8H, *m-H*), 7.30 (d, 8H, *o-H*). ^{13}C NMR (δ) in C_6D_6: 37.06 (NCH_3), 57.67 (PhCH_2), 125.32 (*p-C*), 128.00 (*o-C*), 129.08 (*m-C*), 149.17 (*i-C*).

[{$(PhCH_2)_2N$}$_2$Mg·(HMPA)$_2$] (5). HMPA (20 mmol) was added to a solution of **1** (5 mmol) in 10 mL of toluene, giving a deep red solution. Small block crystals were produced on cooling the solution at −31 °C for 4 h. Yield = 61%. Mp = 81−82 °C. IR (cm^{-1}): 2950 (s), 2875 (s), 2742 (w), 1595 (w), 1460 (m), 1378 (w), 1336 (w), 1301 (w), 1190 (m), 1132 (w), 1063 (w), 992 (m), 970 (m), 959 (w), 755 (w), 728 (m), 699 (w). ^{1}H NMR (δ) in C_6D_6: 2.24 (d, 36H, NCH_3), 4.50 (s, 8H, PhCH_2), 7.22 (t, 4H, *p-H*), 7.36 (t, 8H, *m-H*), 7.79 (d, 8H, *o-H*). ^{13}C NMR (δ) in C_6D_6: 36.80 (NCH_3), 57.45 (PhCH_2), 125.14 (*p-C*), 127.97 (*o-C*), 129.77 (*m-C*), 149.84 (*i-C*).

[{$(PhCH_2)_2N$}$_2$Mg·TMEDA] (6). TMEDA (10 mmol) was added dropwise to a solution of **1** (5 mmol) in 10 mL of toluene with no visible change in the reaction mixture. On cooling of the solution at 0 °C for 24 h, large crystalline blocks were deposited. Yield = 61%. Mp = 140−142 °C. IR (cm^{-1}): 2900 (s), 2782 (m), 2720 (m), 2655 (m), 1595 (w), 1486 (m), 1460 (s), 1378 (w), 1362 (w), 1338 (m), 1310 (m), 1289 (m), 1289 (m), 1256, 1235 (w), 1199 (w), 1180 (w), 1162 (w), 1127 (m), 1066 (m), 1052 (m), 1023 (m), 1010 (w), 965 (w), 956 (w), 900 (w), 796 (m), 730 (s), 700 (s), 650 (w), 594 (w), 552 (w), 480 (w), 433 (w). ^{1}H NMR (δ) in C_6D_6: 1.39 (s, 4H, CH_3CH_2), 1.65 (s, 12H, C$H_3$$CH_2$), 4.28 (s, 8H, PhC$H_2$), 7.21 (t, 4H, *p-H*), 7.40 (t, 8H, *m-H*), 7.69 (d, 8H, *o-H*). ^{13}C NMR (δ) in C_6D_6: 46.51 (NCH_3), 58.38 (PhCH_2), 126.12 (*p-C*), 128.12 (*o-C*), 129.24 (*m-C*), 147.92 (*i-C*).

Crystallographic Studies. Crystals of **1**, **4**, and **6** were mounted onto glass fibers in an oil drop. Data for **1** and **6** were collected on a Stoe-Siemens diffractometer with the structure solutions by direct methods and refinement on F^2.[10] Data for **4** were collected on a Siemens SMART CCD diffractometer. Crystals of **2** and **5** were sealed in glass capillaries under argon, and data were collected on a Rigaku AFC7S diffractometer with the structure solution by direct methods and refinement on F.[11] Both instruments were run using Mo Kα radiation with λ = 0.710 73 Å. The quality of the data solution for **5** was adversely affected by the presence of a severely disordered toluene solvent molecule. After several trial calculations this was modeled as a rigid C_6H_5 group with an occupancy of 50%. The carbon of the

(8) (a) Baker, D. R.; Mulvey, R. E.; Clegg, W.; O'Neil, P. A. *J. Am. Chem. Soc.* **1993**, *115*, 6472. (b) Andrews, P. C.; Armstrong, D. R.; Baker, D. R.; Mulvey, R. E.; Clegg, W.; Horsburgh, L.; O'Neil, P. A.; Reed, D. *Organometallics* **1995**, *14*, 427. (c) Armstrong, D. R.; Davidson, M. G.; Moncrieff, D. *Angew. Chem., Int. Ed. Engl.* **1995**, *34*, 478. (d) Barr, D.; Clegg, W.; Mulvey, R. E.; Snaith, R. *J. Chem. Soc., Chem. Commun.* **1984**, 285. (e) Armstrong, D. R.; Mulvey, R. E.; Walker, G. T.; Barr, D.; Snaith, R.; Clegg, W.; Reed, D. *J. Chem. Soc., Dalton Trans.* **1988**, 617.

(9) Shriver, D. F.; Drezdzon, M. A. *Manipulation of Air Sensitive Compounds*; John Wiley and Sons: New York, 1986.

(10) Sheldrick, G. M. *SHELXTL Manual*; Siemens Analytical Instruments Inc.: Madison, WI, 1990; *SHELXL-93, program for crystal structure refinement, β-test version*; University of Göttingen: Göttingen, Germany, 1992.

(11) Structure solution: Fan, H.-F. *SAPI91, structure analysis program with intelligent control*; Rigaku Corp.: Tokyo, 1991. Calculations and graphics: *Texsan, crystal structure analysis package*, version 1.6; Molecular Structure Corp.: The Woodlands, TX, 1993.

methyl group was placed on two sites, each with an occupancy of 25%, and refined isotropically. Inspection of the thermal displacement parameters also indicates a small amount of further unrefined disorder about one of the HMPA ligands. Atomic coordinates, bond lengths and angles, and displacement parameters have been deposited at the Cambridge Crystallographic Data Centre.

Database Searches. The Cambridge Structural Database was used to determine the mean P−O(HMPA)−M (M = Mg, Li, and any metal) bond angles, the range of Mg−N bond distances, and the mean Mg−O(THF) bond distance for compounds with four-coordinate magnesium.[12] No constraints were used on the searches. The Quest and Vista software packages were used to view the data.

Theoretical MO Calculations. The Gaussian 94 program, revision E.2, was used for the calculations.[13] Initial optimization was carried out using the 6-31G basis set and then reoptimized at the higher 6-31G* level.

Results and Discussion

The following six compounds have been isolated and characterized from the systems studied: [{$(PhCH_2)_2N$}$_2$Mg}$_2$], **1**, [{$(PhCH_2)_2N$}$_2$Mg·THF}$_2$], **2**, [$(PhCH_2)_2N$}$_2$Mg·$(THF)_2$], **3**, [{$(PhCH_2)_2N$}$_2$Mg·HMPA}$_2$], **4**, [$(PhCH_2)_2N$}$_2$Mg·$(HMPA)_2$], **5**, and [$(PhCH_2)_2N$}$_2$Mg·TMEDA], **6**.

Unsolvated compound **1** is readily prepared by the direct reaction of 2 molar equiv of dibenzylamine (DBA) with dibutylmagnesium[14] in toluene solution.[15] The solvates were formed by the addition of donor to *in situ* prepared **1**. Complexes **2**, **4**, and **6** were derived from the addition of 2 molar equiv of donor solvent to the reaction mixture containing **1,** *i.e.* 2 equiv of solvent per dimer of **1**. Similarly, **5** was obtained by increasing the stoichiometry of HMPA solvent to 4 molar equiv. However, on the addition of 4 molar equiv of THF to the reaction mixture, the monosolvated complex **2** was deposited as the sole isolable product. When the THF to **1** ratio was increased further to 20:1, the bis-solvated complex **3** was precipitated, after cooling the solution. Rationalization of the different solvent ratios in the complexes will be detailed in the NMR and X-ray discussion sections below.

NMR Spectroscopic Studies. A good deal of information may be derived from the benzylic CH_2 region of the ^{1}H NMR spectra of the complexes. Starting with **1** as a solution in toluene-d_8, at 298 K a sharp peak on top of two broad humps is seen in the region 2.9−4.0 ppm. A variable-temperature study was carried out on this sample between 188 and 368 K (Figure 1). This revealed that, at subambient temperatures, two distinct benzylic CH_2 signals are present in a 1:1 ratio. Of note is the large difference in chemical shift of the two distinct types of benzylic CH_2, which appear at 3.98 and 2.70 ppm at 248 K. At 188 K, there are two clearly defined signals, A and B, one of which is markedly broader than the other. This, allied to the fact that COSY NMR experiments indicate the signals do not couple to one another, is consistent with two different benzyl CH_2 units (the increased broadness of one of these signals may imply that there is a subsequent coalescence process likely to occur, at even lower temperature, between the geminal protons of one of the benzyl CH_2 units). Coalescence between A and B occurs at 368 K. The integrals of the two benzylic signals were found to be independent of the concentration of the sample. These data are consistent with the solution state species being a dimer, akin to that seen in the previously determined[15] crystal structure of **1**; *i.e.*, the bridging and terminal dibenzylamido units appear as two distinct benzylic CH_2 signals.

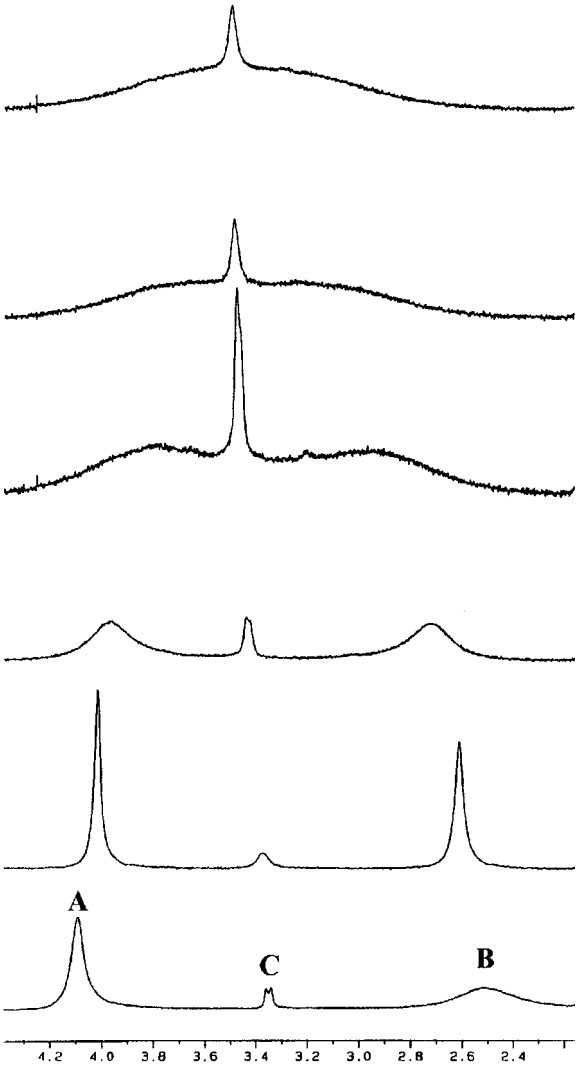

Figure 1. Variable-temperature ^{1}H NMR spectra of **1** showing the benzylic protons present.

Kinetic and thermodynamic information may be elicited from the variable-temperature ^{1}H NMR study of **1**. Assuming the limiting chemical shift difference, $\Delta\nu$, as estimated from the spectrum obtained at 188 K, is 570 (±20) Hz and, since we are dealing with uncoupled exchanging protons, using the equation $k = 2.22\Delta\nu$, we can evaluate k as 1265 s^{-1}. Using the well-established equation

$$\Delta G^* = 19.14T_c[10.32 + \log(T_c/k)]\ \text{J mol}^{-1} \qquad (2)$$

where T_c = 368 (±1) K and k = 1265 s^{-1}, we can evaluate ΔG^* = 66.0 kJ mol^{-1}, or 15.7 kcal mol^{-1}.

Last, for **1**, peak C, which lies between the two broad peaks A and B, is present throughout the variable-temperature study. This peak is assigned to the unsolvated, two-coordinate monomer [{$(PhCH_2)_2N$}$_2$Mg], **7**.[16] Further evidence for the assignment of **7** was found from a concentration study of the bis-

(12) Allen, F. H.; Kennard, O. *Chem. Des. Autom. News* **1993**, 8, 31.
(13) Frisch, M. J.; Trucks, G. W.; Schlegel, H. B.; Gill, P. M. W.; Johnson, B. G.; Robb, M. A.; Cheeseman, J. R.; Keith, T.; Petersson, G. A.; Montgomery, J. A.; Raghavachari, K.; Al-Laham, M. A.; Zakrzewski, V. G.; Ortiz, J. V.; Foresman, J. B.; Cioslowski, J.; Stefanov, B. B.; Nanayakkara, A.; Challacombe, M.; Peng, C. Y.; Ayala, P. Y.; Chen, W.; Wong, M. W.; Andres, J. L.; Replogle, E. S.; Gomperts, R.; Martin, R. L.; Fox, D. J.; Binkley, J. S.; Defrees, D. J.; Baker, J.; Stewart, J. P.; Head-Gordon, M.; Gonzalez, C.; Pople, J. A. *GAUSSIAN 94*; Gaussian, Inc.: Pittsburgh PA, 1995.
(14) Dibutylmagnesium is prepared as a 1:1 ratio of *n*- to *sec*-butyl in heptane.
(15) Compound **1** was previously reported by our group in a communication: Clegg, W.; Henderson, K. W.; Mulvey, R. E.; O'Neil, P. A. *J. Chem. Soc., Chem. Commun.* **1994**, 769.

Scheme 1

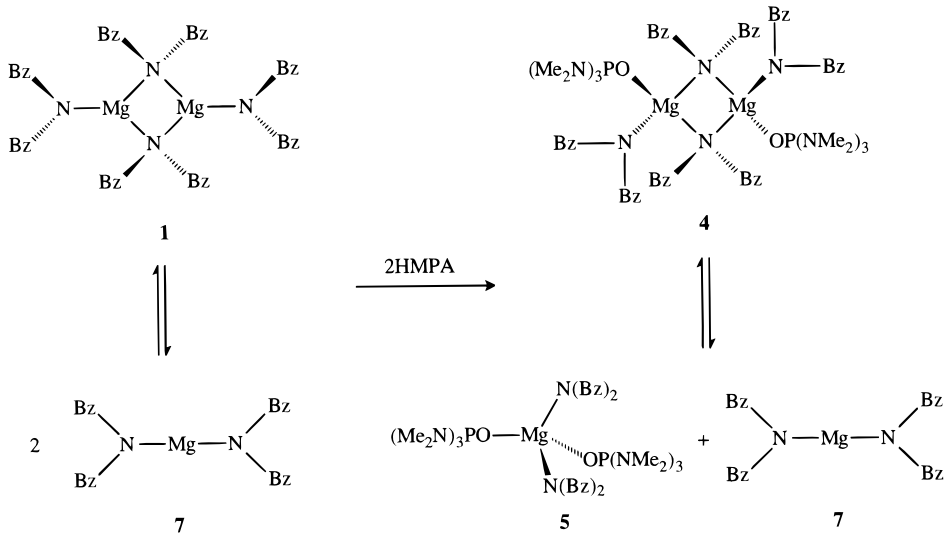

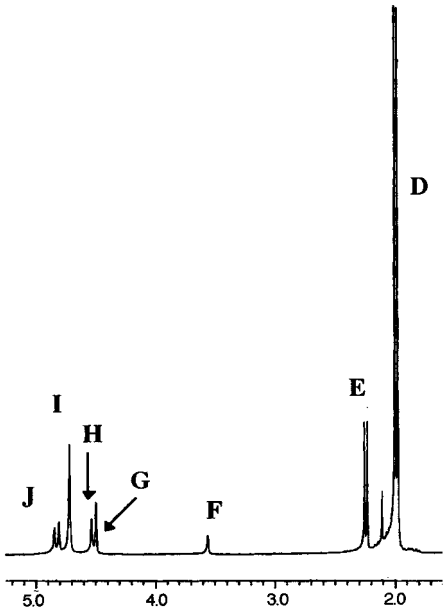

Figure 2. ^{1}H NMR spectrum of a dilute sample of **4** showing the three aggregates present.

solvated dimer **4** (see below).[17] At 188 K, peak C appears to split; this is due to the benzylic CH_2's becoming inequivalent with slower rotation (see theoretical section).

In the ^{1}H NMR spectrum of **4**, the region 4.4−5.0 ppm comprises two doublets at 4.52 and 4.83 ppm (H and J), each of relative area 2, and a singlet (I) of relative area 4 at 4.72 ppm (Figure 2). A COSY experiment determined that the doublets couple with one another, and hence these represent a pair of inequivalent protons attached to a single benzylic carbon. As with **1**, these data are consistent with bridging and terminal dibenzylamido units from a magnesium dimer. It is likely that the doublets correspond to the bridging units since these will have restricted rotation, resulting in inequivalent environments for the hydrogens attached to the benzyl groups. This notion is supported by the presence of two equal-intensity signals at 7.67 and 7.76 ppm, which correspond to different types of *ortho* protons.

A variable-concentration study (1.64×10^{-5}−4.92×10^{-4} g L^{-1}) was conducted on **4** with no effect on the integration ratio of the doublets H and J to the singlet I, again supporting the suggestion of a dimer in solution. However, altering the concentration of the solution has a dramatic effect on the relative ratios of the two HMPA doublets D and E and on the broad singlet F centered at 3.57 ppm. The ratio of the HMPA E and D signals varies between 1:2.2 (low concentration) and 1:14 (high concentration). Neither of these signals corresponds to "free" HMPA, which is centered at 2.41 ppm in C_6D_6. Also, as the concentration decreases, the integral of singlet F increases at the same rate as the integral of doublet E. Additionally, a new singlet G appears at 4.50 ppm, which is obscured by the doublet H at high concentration. Assuming the peaks F and G represent benzylic CH_2 groups, the ratio of the $(PhCH_2)_2N^-$ signal to the HMPA signal E is approximately 1:1, indicating two HMPA ligands per $[\{(PhCH_2)_2N\}_2Mg]$ unit. This pattern can be explained by E and F representing a monomer with two solvating HMPA ligands and G representing an unsolvated monomer. Conformation of these assignments comes from the identical chemical shift positions of E and F compared with those of monomer **5**. Second, the singlet G has a chemical shift similar to that of singlet C in the toluene-d_8 solution of **5**. These assignments are consistent with increasing monomer present at higher dilution. Values of the integrals throughout the concentration range corroborate the assignment of signal D as HMPA associated with the bis-solvated dimer **4**. Therefore, at least three species are simultaneously present in benzene solutions of **4**: a dimer with terminally-coordinated HMPA ligands, a bis-solvated monomer, and an unsolvated monomer (Scheme 1). The complex nature of the solution state of **4** is also seen from the ^{13}C NMR spectrum, which shows a series of overlapping signals for both the benzylic CH_2 groups and the aromatic protons. No evidence exists for a bridging donor, a common coordination mode for HMPA with lithium.[18] ^{1}H NMR spectra of **4** obtained from THF-d_8 solutions show the presence of a single benzylic resonance at 3.97 ppm, most likely indicating deaggregation of the dimer to a solvated monomer.

The ^{1}H NMR spectra of the complexes **3**, **5**, and **6** contain one singlet for the benzylic protons and the three resonances for the phenyl groups, as well as the signals corresponding to the solvent molecules themselves. The appearance of only one set of benzyl signals for these complexes is indicative of all four benzyl units on the magnesium within each compound being in equivalent electronic environments. It should be stated

(16) Concentration studies were limited due to the relatively poor solubility of **1** in nonpolar media.

(17) We previously observed a monomer−dimer equilibrium for the compound $[\{(Me_3Si)_2N\}_2Mg]$: Henderson, K. W.; Allen, J. F.; Kennedy A. R. *J. Chem. Soc.,Chem. Commun.* **1997**, 1149 .

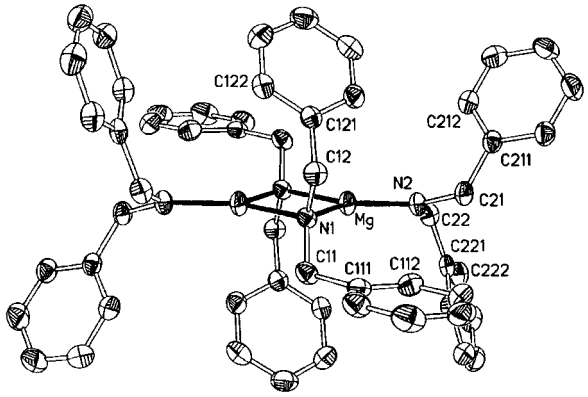

Figure 3. Molecular structure of **1** with 50% probability ellipsoids and with hydrogen atoms omitted for clarity.

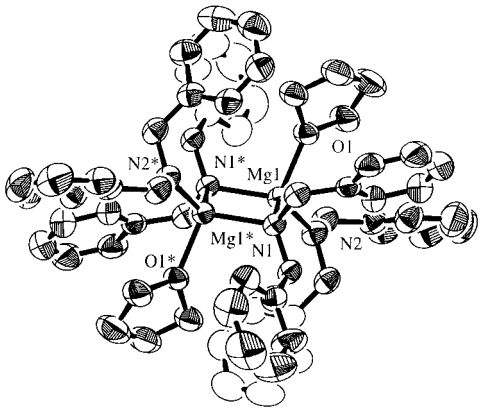

Figure 4. Molecular structure of **2** with 40% probability ellipsoids and with hydrogen atoms omitted for clarity.

that the NMR spectra of the THF complex **2** did not show two distinct types of benzyl signals as would be expected for a dimer. In this instance, the aggregation state of **2** in arene solution cannot be ascertained.

X-ray Structure Data. Single-crystal analyses were carried out on compounds **1**, **2**, **4**, **5**, and **6** (molecular structures are shown in Figures 3−7, key bond lengths and angles are detailed in Tables 1−5, and a summary of the crystallographic data is given in Table 6). Three structural types were revealed, bis-solvated monomers (**5** and **6**; bis-solvation in **6** is taken as chelation from TMEDA), bis-solvated dimers (**2** and **4**), and an unsolvated dimer (**1**). Also, compound **5** crystallizes with a

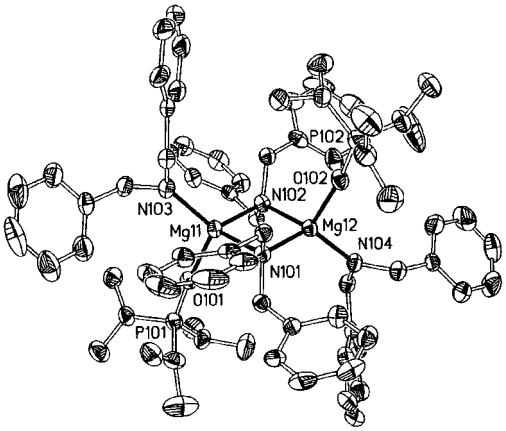

Figure 5. Molecular structure of one dimer from the structure of [**4**·1.5toluene] with 50% probability ellipsoids and with hydrogen atoms omitted for clarity.

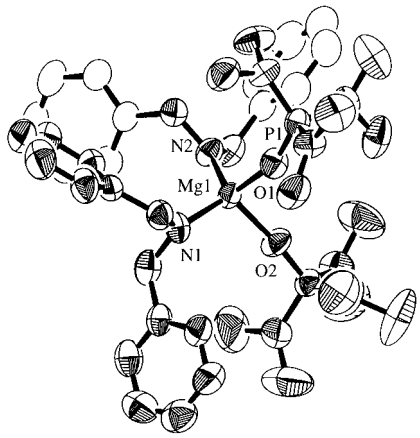

Figure 6. Molecular structure of the monomer fragment of [**5**·0.5toluene] with 40% probability ellipsoids and with hydrogen atoms omitted for clarity.

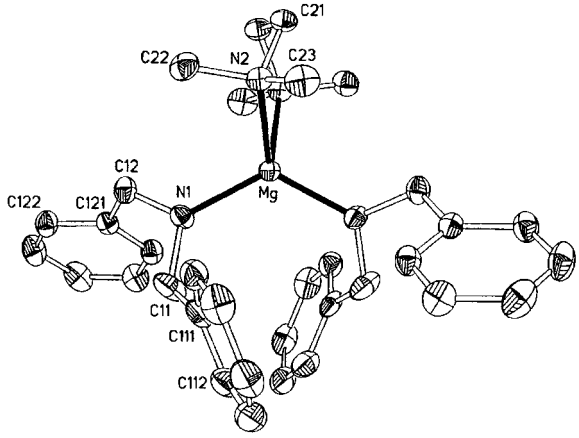

Figure 7. Molecular structure of **6** with 50% probability ellipsoids and with hydrogen atoms omitted for clarity.

half-molecule of toluene in its asymmetric unit, resulting in a unit cell containing two monomers and one toluene.

To our knowledge, this is the first crystallographic characterization of a magnesium amide to show aggregation dependency on the donor solvent stoichiometry. In fact, variable aggregation for other early main group organometallics effected by altering the amount of donor solvent present has only rarely been confirmed in the solid state.[19] In comparison, numerous solution studies of organolithium species have revealed highly complex equilibria being critically dependent on the amount and nature of the solvent present. For example, NMR spec-

(18) (a) Barr, D.; Clegg, W.; Mulvey, R. E; Snaith, R. *J. Chem. Soc., Chem. Commun.* **1984**, 700. (b) Barr, D.; Clegg, W.; Mulvey, R. E.; Snaith, R. *J. Chem. Soc., Chem. Commun.* **1984**, 974. (c) Barr, D.; Doyle, M. J.; Drake, S. R.; Raithby, P. R.; Snaith, R.; Wright, D. S. *J. Chem. Soc., Chem. Commun.* **1988**, 1415. (d) Jens, K.; Kopf, J.; Lorenzen, N. P.; Weiss, E. *Chem. Ber.* **1988**, *121*, 1201. (e) Armstrong, D. R.; Mulvey, R. E.; Barr, D.; Porter, R. W.; Raithby, P. R.; Simpson, T. R. E.; Snaith, R.; Wright, D. S.; Gregory, K.; Mikulcik, P. *J. Chem. Soc., Dalton Trans.* **1991**, 765. (f) Raithby, P. R.; Reed, D.; Snaith, R.; Wright, D. S. *Angew. Chem., Int. Ed. Engl.* **1991**, *30*, 1011. (g) Armstrong, D. R.; Banbury, F. A.; Cragg-Hine, I.; Davidson, M. G.; Mair, F. S.; Pohl, E.; Raithby, P. R.; Snaith, R. *Angew. Chem., Int. Ed. Engl.* **1993**, *32*, 1769. (h) Armstrong, D. R.; Barr, D.; Brooker, A. T.; Clegg, W.; Gregory, K.; Hodgson, S. M.; Snaith, R.; Wright, D. S. *Angew. Chem., Int. Ed. Engl.* **1990**, *29*, 410. (i) Hyvarinen, K.; Klinga, M.; Leskela, M. *Polyhedron* **1996**, *15*, 2171. (j) Barr, D.; Doyle, M. J.; Mulvey, R. E.; Raithby, P. R.; Reed, D.; Snaith, R.; Wright, D. S. *J. Chem. Soc., Chem. Commun.* **1989**, 318. (k) Armstrong, D. R.; Mulvey, R. E.; Barr, D.; Snaith, R.; Wright, D. S.; Clegg, W.; Hodgson, S. M. *J. Organomet. Chem.* **1989**, *362*, C1. (l) Armstrong, D. R.; Banbury, F. A.; Davidson, M. G.; Raithby, P. R.; Snaith, R.; Stalke, D. *J. Chem. Soc., Chem. Commun.* **1992**, 1492. (m) Mair, F. S.; Scully, D.; Edwards, A. J.; Raithby, P. R.; Snaith, R. *Polyhedron* **1995**, *14*, 2397.

Table 1. Selected Bond Lengths (Å) and Angles (deg) for [{$(PhCH_2)_2N$}$_2$Mg}$_2$], **1**

Mg1−N1	2.077(2)	Mg1−N2	1.935(2)
Mg1−N1[a]	2.100(2)		
N1−Mg1−N2	135.51(6)	N1[a]−Mg1−N2	130.23(6)
N1−Mg−N1[a]	94.22(5)	Mg1−N1−Mg1[a]	113.56(10)
C11−N1−C12	109.28(13)	C11−N1−Mg1	121.67(11)
C11−N1−Mg1[a]	113.56(10)	C12−N1−Mg1	112.77(10)
C12−N1−Mg1[a]	111.92(10)	C22−N2−Mg1	121.90(11)
C22−N1−Mg1	126.25(11)		

[a] $1 - x, -y, -z$.

Table 2. Selected Bond Lengths (Å) and Angles (deg) for [{$(PhCH_2)_2N$}$_2$Mg·THF}$_2$], **2**

Mg1−O1	2.070(2)	Mg1−N1	2.139(2)
Mg1−N1[a]	2.132(2)	Mg1−N2	2.006(2)
O1−Mg1−N1	108.36(8)	O1−Mg1−N1[a]	103.74(8)
O1−Mg1−N2	107.91(9)	N1−Mg1−N1[a]	91.77(8)
N1−Mg1−N2	117.63(9)	N1[a]−Mg1−N2	125.51(9)
Mg1−N1−Mg1[a]	88.23(8)	Mg1−N1−C1	116.6(1)
Mg1−N1−C8	112.1(2)	Mg1[a]−N1−C8	112.2(2)
C1−N1−C8	109.4(2)	Mg1−N2−C15	121.4(2)
Mg1−N2−C22	127.5(2)	C15−N2−C22	110.2(2)
Mg1−O1−C29	123.1(2)	Mg1−O1−C32	132.2(2)
C29−O1−C32	104.7(2)		

[a] $1 - x, 1 - y, 1 - z$.

Table 3. Selected Bond Lengths (Å) and Angles (deg) for One of the Independent Dimers of [{$(PhCH_2)_2N$}$_2$Mg·HMPA}$_2$], **4**

Mg11−N101	2.137(3)	Mg11−N102	2.142(3)
Mg11−N103	2.009(3)	Mg12−N101	2.122(3)
Mg12−N102	2.147(3)	Mg12−N104	1.990(3)
Mg11−O101	1.999(2)	Mg12−O102	2.147(3)
O101−Mg11−N103	108.45(12)	O101−Mg11−N101	105.20(11)
N103−Mg11−N101	122.16(12)	O101−Mg11−N102	110.57(11)
N103−Mg11−N102	117.91(12)	N101−Mg11−N102	91.09(11)
N104−Mg12−O102	106.80(11)	N104−Mg12−N101	123.92(12)
O102−Mg12−N101	104.32(11)	N104−Mg12−N102	117.58(12)
O102−Mg12−N102	111.74(11)	N101−Mg12−N102	91.39(11)
P101−O101−Mg11	171.40(16)	P102−O102−Mg12	170.86(16)
C101−N010−C108	111.0(3)	C101−N101−Mg12	112.5(2)
C108−N101−Mg12	115.0(2)	C101−N101−Mg11	115.1(2)
C108−N101−Mg11	112.7(2)	Mg12−N101−Mg11	89.14(11)
C122−N102−C115	110.2(3)	C122−N102−Mg11	115.9(2)
C115−N102−Mg11	111.9(2)	C122−N102−Mg12	105.61(19)
C115−N102−Mg12	123.7(2)	Mg11−N102−Mg12	88.37(11)
C136−N103−C129	109.9(3)	C136−N103−Mg11	124.9(2)
C129−N103−Mg11	124.9(2)	C143−N104−Mg12	126.2(2)
C143−N104−Mg12	122.4(2)	C150−N104−Mg12	126.2(2)

troscopic studies show that addition of HMPA to lithium salts can increase the aggregation state,[20] produce solvent-separated species,[21] or have no overall effect on the aggregation state.[22]

Since magnesium complexes **1**, **2**, and **4**−**6** are all derived from the same parent amine, this allows for a detailed comparative study of their structural features. Averaged values are used where appropriate without estimated standard deviations.

Table 4. Selected Bond Lengths (Å) and Angles (deg) for [{$(PhCH_2)_2N$}$_2$Mg·2HMPA], **5**

Mg1−O1	1.975(4)	Mg1−O2	1.967(3)
Mg1−N1	1.980(5)	Mg1−N2	1.976(4)
O1−Mg1−O2	99.7(1)	O1−Mg1−N1	104.9(2)
O1−Mg1−N2	114.0(2)	O2−Mg1−N1	113.6(2)
O2−Mg1−N2	104.2(2)	N1−Mg1−N2	118.9(2)
Mg1−N1−C1	119.1(3)	Mg1−N1−C8	129.8(4)
C1−N1−C8	110.8(4)	Mg1−N2−C15	127.2(3)
Mg1−N2−C22	110.2(4)	P1−O1−Mg1	158.2(2)
P2−O2−Mg1	172.3(3)		

Table 5. Selected Bond Lengths (Å) and Angles (deg) for [{$(PhCH_2)_2N$}$_2$Mg·TMEDA], **6**

Mg1−N1	1.978(2)	Mg1−N2	2.236(2)
N1−Mg1−N1[a]	124.75(12)	N1−Mg−N2[a]	115.01(7)
N1−Mg1−N2	106.04(8)	N2−Mg1−N2[a]	82.15(10)
C11−N1−C12	109.6(2)	Mg1−N1−C12	125.0(2)
Mg1−N1−C11	124.8(2)		

[a] $-x, y, {}^1/_2 - z$.

It should be mentioned that complex **4** adopts a highly unusual crystalline form, with a large unit cell volume of 21178.4(15) Å^3. Data for this crystal were collected on a CCD area detector diffractometer, and over 88 000 reflections were recorded overnight. The asymmetric unit contains three independent dimers and 1.5 molecules of toluene ($Z = 12$ in $P2_1/c$), which leads to the unusually large unit cell. Discussion of **4** will concentrate on one of the independent dimers, since the others have essentially identical geometric parameters.

Starting with the anionic nitrogen to magnesium bonds, we note the sequence of increasing Mg−N bond lengths as follows: the terminal anion in **1** at 1.935(2) Å, the two monomers **5** and **6** at 1.978 Å, the terminal anions in the solvated dimers **2** and **4** at 2.002 Å, the bridging anions in **1** at 2.088 Å, and, last, the bridging anions in the solvated dimers **2** and **4** at 2.136 Å. This range of bond lengths covering 0.201 Å can be rationalized in terms of the local bonding environment at magnesium. In **1**, the magnesium is tricoordinate, and in the remaining complexes, magnesium is tetracoordinate. The lower coordination number of the metal in **1** leads to shorter, stronger bonding with both anions (an even lower coordination number of 2 is implicated in arene solutions of **1** and **4**, where unsolvated monomer **7** is present). As a consequence, the terminal and bridging ligands in **1** have significantly shorter bonds than those in the solvated dimers. In fact, **1** has a shorter Mg−N distance than any analogous distances found at present in the Cambridge Structural Database (CSD).[12] This is perhaps surprising, considering that a two-coordinate magnesium amide, [{$(MePh_2Si)_2N$}$_2$Mg], **8**, has been structurally characterized (Mg−N 1.968 Å).[23] Repulsion of the highly positive magnesium by the silicons of the amide, coupled with steric repulsions between the bulky ligands, is the probable cause of the longer bonding in **8** compared to **1**. The bridging Mg−N bonds in **1** are longer than the terminal ones in the monomers **5** and **6** in spite of the lower coordination number at the metal. In this instance, the sharing of the anionic linkages in the dimer **1** weakens the local bonding; *i.e.*, the bonding of each bridging anion in **1** is spread over two metal centers as opposed to only one in the monomers **5** and **6**, leading to an increase in the bond lengths.

The N(anion)−Mg−N(anion) angles in monomers **5** and **6** are 118.9 and 124.75°, respectively. The larger angle for **6** is

(19) For example, two THF solvates of lithium anilide are known: (a) Clegg, W.; Horsburgh, L.; Mackenzie, F. M.; Mulvey, R. E. *J. Chem. Soc., Chem. Commun.* **1995**, 2011. (b) Von Bülow, R.; Gornitzka, H.; Kottke, T.; Stalke, D. *J. Chem. Soc., Chem. Commun.* **1996**, 1639.
(20) Jackman, L. M.; Chen, X. *J. Am. Chem. Soc.* **1992**, *114*, 403.
(21) (a) Reich, H. J.; Green, D. P.; Phillips, N. H. *J. Am. Chem. Soc.* **1989**, *111*, 3444. (b) Reich, H. J.; Green, D. P. *J. Am. Chem. Soc.* **1989**, *111*, 8729. (c) Reich, H. J.; Borst, J. P. *J. Am. Chem. Soc.* **1991**, *113*, 1835. (d) Reich, H. J.; Medina, M. A.; Bowe, M. D. *J. Am. Chem. Soc.* **1992**, *114*, 11003. (e) Reich, H. J.; Borst, J. P.; Dykstra, R. R.; Green, P. D. *J. Am. Chem. Soc.* **1993**, *115*, 8728.
(22) (a) Romesberg, F. E.; Bernstein, M. P.; Gilchrist, J. H.; Harrison, A. T.; Fuller, D. J.; Collum, D. B. *J. Am. Chem. Soc.* **1993**, *115*, 3475. (b) Romesberg, F. E.; Gilchrist, J. H.; Harrison, A. T.; Fuller, D. J.; Collum, D. B. *J. Am. Chem. Soc.* **1991**, *113*, 5751. (c) Romesberg, F. E.; Collum, D. B. *J. Am. Chem. Soc* **1994**, *116*, 9187. (d) Romesberg, F. E.; Collum, D. B. *J. Am. Chem. Soc* **1994**, *116*, 9198.
(23) Bartlett, R. A.; Olmstead, M. M.; Power, P. P. *Inorg. Chem.* **1994**, *33*, 4800.

Table 6. Crystallographic Data

	1	**2**	**4**	**5**	**6**
empirical formula	$C_{56}H_{56}Mg_2N_4$	$C_{64}H_{72}Mg_2N_4O_2$	$C_{71.5}H_{98}Mg_2N_{10}O_2P_2$	$C_{43.5}H_{68}MgN_8O_2P_2$	$C_{34}H_{44}MgN_4$
fw	833.6	977.9	1240.2	821.3	533.0
space group	$P2_1/c$	$P2_1/n$	$P2_1/c$	$P\bar{1}$	$C2/c$
a, Å	9.943(2)	11.821(3)	14.7440(6)	11.494(3)	10.052(2)
b, Å	15.813(3)	19.843(4)	21.4484(8)	11.857(2)	14.698(3)
c, Å	14.559(2)	12.464(2)	66.996(3)	18.732(3)	20.514(4)
α, deg				80.24(1)	
β, deg	97.57(2)	106.57(1)	91.588(2)	87.54(2)	95.50(2)
γ, deg				73.06(2)	
V, Å^3	2269.1(7)	2802.3(8)	21178.4(15)	2406.7(8)	3016.9(10)
Z	2	2	12	2	4
ρ_{obsd}, g cm^{-3}	1.220	1.159	1.167	1.133	1.174
μ, cm^{-1}	0.96	0.84	1.30	1.45	0.88
T, °C	−78	17	−118	17	−118
R^a	0.039	0.041	0.065	0.073	0.042
$R_w{}^b$	0.128	0.048	0.153	0.095	0.134

[a] Conventional $R = \sum||F_o| - |F_c||/\sum|F_o|$ for "observed" reflections having $F_o^2 > 2\sigma(F_o^2)$. [b] $R_w = [\sum w(F_o^2 - F_c^2)^2/\sum w(F_o^2)^2]^{1/2}$ for all data for compounds **1**, **4**, and **6**; $R_w = [\sum w(F_o - F_c)^2/\sum wF_o^2]^{1/2}$ for "observed" reflections for compounds **2** and **5**.

due to the fixed chelation "bite size" of TMEDA allowing the two anions more coordination freedom than in **5**.

For the dimers, the N(terminal)−Mg−N(bridging) angles are smaller for the solvate **2** at 121.57° and the solvate **4** at 120.39° than for **1** at 132.87°. This is caused by the incorporation of donor ligands in **2** and **4**, which moves the terminal anions out of the plane of the dimeric ring, into a more regular tetrahedral position about the magnesium centers (averaged angles at magnesium are 109.2° for both **2** and **4** and 120.0° for **1**). Overall there is a change from pseudo-trigonal-planar magnesium geometry in **1**, to pseudo-tetrahedral geometry in the solvates **2** and **4**. Another structural effect of solvation is the rearrangement of the bridging benzyl groups. In **1**, one phenyl ring from each of the bridging anions is tilted over the plane of the dimeric ring. Upon solvation, both benzyl groups twist away from the dimeric ring, illustrating the flexibility of this ligand.

Turning to the Mg−O(HMPA) bond lengths in compounds **4** and **5**, an interesting pattern is seen. The Mg−O bonds in dimer **5** are 0.025 Å longer than those in monomer **4**. Surprisingly, there are only three previously reported magnesium complexes containing coordinated HMPA, namely [{PhNMg·HMPA}$_6$], **9**,[24] [{1,8-(NH)$_2$C$_{12}$H$_6$Mg·HMPA}$_3$], **10**,[25] and [{MesN(H)}$_2$Mg·(HMPA)$_2$], **11**,[26] which hinders a direct comparison of expected bond lengths for these systems. However, our laboratory has prepared two magnesium complexes containing HMPA as ligand, the bimetallic "ate" species [Mg(HMPA)$_4$·2AlMe$_4$], **12**, and the amide dimer [{PhCH$_2$N(H)EtN(H)CH$_2$PhMg·HMPA}$_2$], **13**.[27] The complexes have averaged Mg−O(HMPA) bond lengths at 1.963, 1.926, 1.972, 1.840, and 1.938 Å for **9**−**13** respectively. The best comparison with the dibenzylamido complexes is with **13**, since it is also a bis(amide) (singly deprotonated at two amine sites within the same molecule) and is dimeric with terminal HMPA units. The large difference in Mg−O bond length (0.058 Å) between the closely analogous dimers **4** and **13** may be caused by steric influences. In **13**, only two amide ligands per dimer are present, whereas **4** contains four. The concomitant increase in steric bulk of the ligand system around **4** allows for only relatively weak solvation of the dimer by HMPA (Mg−O 1.996 Å).[28] In **2**, the Mg−O distance of 2.070(2) Å is also slightly elongated compared to the mean four-coordinate Mg−O(THF) distance of 2.046 Å found in the CSD.

Analysis of the P−O−Mg angles in **4**, **5**, and **9**−**13** show a large variation spanning 151.2−174.8°. In the sterically crowded dimer **4**, the average P−O−Mg angle is 171.1° whereas, in **13**, the angle is 161.5°. Two distinct P−O−Mg angles are apparent in monomers **5** and **11** (158.2(2) and 172.3(3)° for **5**; 157.6(5) and 173.1(6)° for **11**). Similarly, in **9** there are three independent P−O−Mg angles at 174.5, 174.8, and 162.8°. Even more dramatically, the three independent P−O−Mg angles in trimer **10** are 151.2(2), 167.5(2), and 171.0(2)°, illustrating versatile bonding modes of HMPA in these systems. The mean P−O−M (M = any metal) angle for terminally bound HMPA found in the CSD is 156.5°, which is as expected for coordination of a phosphine oxide to a metal. However, an analysis of the modes of HMPA coordination to lithium shows a very even spread of P−O−Li angles in the range 140−180°, with no obvious preference for the angle of ligation. This is in keeping with the ionic representation of the HMPA ligand as $(Me_2N)_3P^+-O^-$, which is one reason for the preference of μ_2- and μ_3-bridging HMPA in many complexes.[18] There is also no clear correlation between P−O−Li angle and Li−O bond length, suggesting that the mode of HMPA coordination to lithium has little effect on the strength of solvation. Therefore, the P−O−M angle for HMPA coordination to a highly electropositive metal such as lithium or magnesium is determined by the local steric environment surrounding the ligand. This is consistent with our observations of the variability of this angle between, and even within, the HMPA solvates of magnesium. For example, the two HMPA ligands in monomer **5** adopt P−O−Mg angles of 158.2(2) and 172.3(3)°, with corresponding and similar Mg−O bond lengths of 1.975(4) and 1.967(3) Å. Again the best comparison of the influence of sterics on ligand coordination in dimer **4** is with dimer **13**. Under the reduced steric conditions in **13**, the HMPA ligand adopts the P−O−Mg angle of 161.5°; in **4**, the more crowded environment only allows for coordination of the ligand by a more nearly linear interaction of 171.13° with the metal.

Three-coordinate magnesium is relatively rare, with only a handful of structures having been elucidated;[29] usually magne-

(24) Grigsby, W. J.; Hascall, T.; Ellison, J. J.; Olmstead, M. M.; Power, P. P. *Inorg. Chem.* **1996**, *35*, 3254.
(25) Clegg, W.; Horsburgh, L.; Mulvey, R. E.; Rowlings, R. *J. Chem. Soc., Chem. Commun.* **1996**, 1739.
(26) Olmstead, M. M.; Grigsby, W. J.; Chacon, D. R.; Hascall, T.; Power, P. P. *Inorg. Chim. Acta* **1996**, *251*, 273.
(27) Clegg, W.; Horsburgh, L.; Mulvey, R. E.; Rowlings, R. Unpublished results.

(28) It should be noted that two of the three independent dimers in the structure of **4** have similar Mg−O bond distances averaged at 1.995 Å with a range of 0.008 Å; however, the other dimer has slightly shortened Mg−O bonds at 1.978 and 1.972 Å, which are similar to those in monomer **5** but still significantly different from those of dimer **12**.

Scheme 2

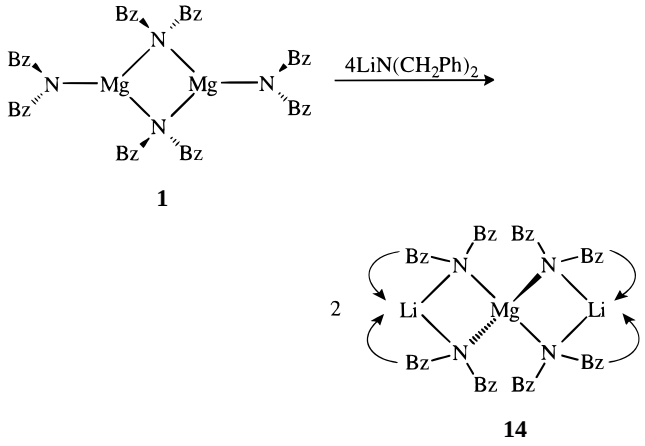

sium is at least four-coordinate.[30] To attain tetracoordination, **1** would have to form a polymer with bridging anions similar to the structures of $[(Me_2Mg)_\infty]$,[31] $[(Et_2Mg)_\infty]$,[31] and $[(Ph_2Mg)_\infty]$.[32] The steric bulk of the anions in **1** precludes this possibility, since four dibenzylamido units would have to surround each metal center. Therefore, a dimer with tricoordinate magnesium is the preferred aggregation state. We have previously shown that tetracoordination of magnesium by the dibenzylamido anion is possible in the complex $[\{(PhCH_2)_2N\}_4MgLi_2]$, **14**.[15] In **14**, the strongly polarizing lithium cations are formally only two-coordinate and pull the benzyl groups away from the central metal, reducing the steric component at magnesium (Scheme 2).

***Ab Initio* Calculations.** X-ray data have been obtained for the unsolvated dimer **1**, the bis-solvated dimers **2** and **4**, and the bis-solvated monomers **5** and **6**. This leaves the unsolvated monomer **7** as the only compound in the series to evade full structural characterization. Since crystallographic analysis of monomer **7** is unlikely, we performed *ab initio* geometry optimization calculations to gain information on its probable structure.[13] Calculations were initially done at the HF/6-31G level and then reoptimized at HF/6-31G*. The starting geometry capped magnesium on either side by a benzyl group from each anion, with the remaining two benzyls directed away from the metal in approximate C_{2h} symmetry. In fact, the preferred geometry was found to be that where two benzyl units were directed to the same face of the metal, with diminished C_2 symmetry. This results in a nonlinear N−Mg−N bond angle of 162.18°. The C_{2h} conformation is of higher energy due to the imposed short contact distance between the CH_2 of one anion and the phenyl ring directed toward the metal of the opposing anion. Therefore, there are less steric interferences when both benzyl rings attracted to the metal tilt toward one another.

Figure 8 shows a structural representation of the optimized geometry of **7A**, and Table 7 lists its key bond lengths and angles (HF = −1385.143 749 2 hartrees). One benzyl group from each of the dibenzylamido anions faces toward the metal center. This leads to short contacts between the benzylic CH_2 and the *ortho*-C with magnesium, which is consistent with these

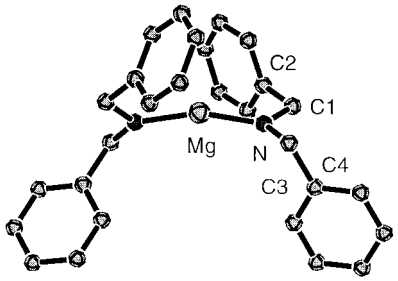

Figure 8. *Ab initio* geometry optimized structure of **7A**.

Table 7. Important Bond Lengths (Å) and Angles (deg) for **7A**

Mg−N	1.938	Mg−C1	2.861
Mg−C2	2.759		
N−Mg−N	162.18	Mg−N−C1	114.58
Mg−N−C3	132.22	N−C1−C2	108.61
N−C3−C4	115.78		

interactions contributing to the overall bonding. All other Mg−C contacts are >3 Å. Numerous short Li−benzyl contacts were located from the structural determination of the lithium amide ring-trimer $[\{(PhCH_2)_2NLi\}_3]$ **15**.[33] Solution studies of **15** indicate the presence of a monomer−trimer equilibrium, contrasting with the monomer−dimer equilibrium found for **1**.[34] A recent calculation on the $(PhCH_2)_2NLi$ monomer at the HF/6-31G* level found that both benzyl groups of the anion tilt toward the lithium.[35] Short Li−benzyl contacts were noted for Li−CH_2 at 2.846 Å and Li−C(*ipso*) at 2.899 Å. In comparison, the Mg−CH_2 and Mg−C(*ipso*) distances are 2.861 and 2.759 Å, respectively, in **7A**. The metal−C(*ipso*) distance in **7A** is significantly shorter in spite of the coordination number of 2 for magnesium compared to 1 for lithium. The reason for shorter Mg−C(*ipso*) contacts lies in the greater Lewis acidity of magnesium compared to lithium, *i.e.* +2 cation *vs* +1 cation with similar ionic radii for both metals.

The ^{1}H NMR spectrum of **1** at 118 K shows the signal representing monomer **7** beginning to split (peak C in Figure 1). This agrees with the optimized geometry of **7A**, since attraction of one benzyl group from each anion toward magnesium renders the CH_2 groups inequivalent.

Conclusions. A combination of NMR, X-ray, and theoretical data has been used to elucidate the nature of the bis(dibenzylamido)magnesium system. Crystalline **1** is dimeric, with three-coordinate magnesium, and the ^{1}H NMR spectra indicate that this aggregation state is retained in arene solution but is in equilibrium with the two-coordinate monomer **7**. Coordinative unsaturation of magnesium in **1** leads to the terminal Mg−N bonds being very short (1.935(2) Å).

Solvation of the metal center by THF or HMPA (**2** or **4**) is possible with retention of the dimeric framework, giving coordination expansion at magnesium.[15] The ^{1}H NMR spectra of the HMPA complex **4** indicate that the dimer is intact in arene solution but that an equilibrium is present with the bis-solvated monomer **5** and the unsolvated monomer **7**. Weak solvation by HMPA in **4** is suggested by the relatively long Mg−O(HMPA) bonds and the nearly linear P−O−Mg bond angles. Nevertheless, the bis(dibenzylamido)magnesium system has shown that the coordination number of the metal can be increased to 4 without changing the aggregation state.

(29) Two other three-coordinate magnesium amide dimers have been structurally characterized; see ref 26 and: Westerhausen, M.; Schwarz, W. *Z. Anorg. Allg. Chem.* **1992**, *609*, 39.
(30) For a review of magnesium structural chemistry, see: Markies, P. R.; Akkerman, O. S.; Bickelhaupt, F.; Smeets, W. J. J.; Spek, A. L. *Adv. Organomet. Chem.* **1991**, *32*, 147.
(31) (a) Weiss, E. *J. Organomet. Chem.* **1964**, *2*, 314. (b) Weiss, E. *J. Organomet. Chem.* **1965**, *4*, 101.
(32) Spek, A. L.; Schat, G.; Akkerman, O. S.; Bickelhaupt, F.; Smeets, W. J. J.; Van der Sluis, P.; Spek, A. L. *J. Organomet. Chem.* **1990**, *393*, 315.
(33) Barr, D.; Clegg, W.; Mulvey, R. E.; Snaith, R. *J. Chem. Soc., Chem. Commun.* **1984**, 285.
(34) Armstrong, D. R.; Mulvey, R. E.; Walker, G. T.; Barr, D.; Snaith, R.; Clegg, W.; Reed, D. *J. Chem. Soc., Dalton Trans.* **1988**, 617.
(35) Armstrong, D. R.; Baker, D. R.; Craig, F. J.; Mulvey, R. E.; Clegg, W.; Horsburgh, L. *Polyhedron* **1996**, *15*, 3533.

Increasing the stoichiometry of donor present alters the aggregation state of the resultant complexes. Addition of 4 equiv of HMPA and 2 equiv of TMEDA to **1** affords the bis-solvated monomeric crystalline complexes **5** and **6**, respectively. However, a large excess of THF is needed to force deaggregation of the dimer to bis-solvated **3**, which is most likely a monomer akin to **5**. The need for excess THF to give the bis-solvate is probably a function of the smaller solvation energy of THF compared to HMPA, *i.e.*, the stronger donor more easily deaggregates the dimer.[36] The ^{1}H and ^{13}C NMR spectra of **3**, **5**, and **6** are consistent with only a single aggregation state, that of the monomers, being present in arene solution.

In summary, the aggregation state of the bis(dibenzylamido)-magnesium system is critically determined by several factors: (i) the presence/absence of donor solvent, (ii) the relative strength of the solvent, (iii) the stoichiometry of solvent present, (iv) the concentration of the solution, and (v) the denticity of the solvent. Only by taking account all of these considerations can we reasonably predict the state of association for the complex. Using the information from this study, it should be possible to predict the aggregation for other bis(amido)-magnesium compounds. This may be of use when mechanistic details of transformations using these compounds as reagents are considered.

Acknowledgment. We thank the Royal Society for granting K.W.H. a University Research Fellowship and the EPSRC for funding P.A.O. and F.J.C. on studentships and for an equipment grant (W.C.).

Supporting Information Available: Four X-ray crystallographic files, in CIF format, are available on the Internet only. Access information is given on any current masthead page.

IC970912A

(36) (a) Lucht, B. L.; Bernstein, M. P.; Remenar, J. F.; Collum, D. B. *J. Am. Chem. Soc.* **1996**, *118*, 10707. (b) Lucht, B. L.; Collum, D. B *J. Am. Chem. Soc.* **1996**, *118*, 2217.